Journal of Science and Technology in Civil Engineering, NUCE 2021. 15 (1): 67–78

A 3-D FINITE ELEMENT MODELING FOR THE TEXTILE-REINFORCED CONCRETE PLATES UNDER TENSILE LOAD USING A NON-LINEAR BEHAVIOUR FOR CEMENTITIOUS MATRIX

Tran Manh Tien[a,*], Xuan Hong Vu[b], Dao Phuc Lam[c], Pham Duc Tho[d]

[a]*Department of Mechanisms of Materials, Hanoi University of Mining and Geology (HUMG), 18 Pho Vien street, Bac Tu Liem district, Hanoi, Vietnam*
[b]*Université de LYON, Université Claude Bernard LYON 1, Laboratoire des Matériaux Composites pour la Construction LMC2, France*
[c]*Faculty of Civil Engineering, Hanoi University of Transport Technology, 54 Trieu Khuc street, Thanh Xuan district, Hanoi, Vietnam*
[d]*Faculty of Construction, Hanoi University of Mining and Geology (HUMG), 18 Pho Vien street, Bac Tu Liem district, Hanoi, Vietnam*

Article history:
Received 18/11/2020, Revised 02/01/2021, Accepted 11/01/2021

Abstract

A big question in the numerical approaches for the mechanical behavior of the textile-reinforced concrete (TRC) composite under tensile loading is how to model the cracking of the cementitious matrix. This paper presents numerical results of 3-D modeling of TRC composite in which the non-linear behavior model was used by considering the cracking for the cementitious matrix. The input data based on the experimental results in the literature. As numerical results, the TRC composite provides a strain–hardening behavior with three phases in which the second one is characterized by the drops in stress on the stress-strain curve. Furthermore, this model could show the failure mode of the TRC specimen with the multi-cracking on its surface after the numerical tests. From this model, the development of a crack from micro-crack to macro at a cross-section was highlighted. The stress jumps in reinforcement textile after each crack was also observed and analyzed. In comparison with the experiment, a good agreement between both results was found for all cases of this study. A parametric study could show the effect of the length and position of the measurement zone on the stress-strain curve of TRC's mechanical behavior.

Keywords: textile reinforced concrete (TRC); cementitious matrix; textile reinforcement; mechanical behaviour; numerical modeling.

https://doi.org/10.31814/stce.nuce2021-15(1)-06

1. Introduction

In the world, the textile (or fiber) reinforced concrete composite (TRC or ECC) has been increasingly and widely applied in the civil engineering field. In Vietnam, they were studied and used as reinforced materials in special cases of structures [1]. As presented in previous research of authors'

*Corresponding author. *E-mail address:* tranmanhtien@humg.edu.vn (Tien, T. M.)

team [2, 3], to consider all effects of the factors belonging to the reinforcement textile or the cementitious matrix on TRC material behavior in tensile, a single experimental approach is not feasible due to issues of time and cost. Therefore, the numerical approach is a reasonable choice for this studying. The global behaviour of TRC material can be predicted using a mesoscale numerical model with the input data of the constitutive materials (reinforcement textile, cementitious matrix, and textile/matrix interface). The local behavior of the constitutive materials can also be studied from this numerical model.

In the literature, there were several numerical studies on the mechanical behavior of TRC composite materials. Portal et al. [4] presented 2-D modeling of the flexural behavior of a carbon TRC thin plate specimen. In this research, the sensitivity of the contact perimeter between carbon textile yarns and cementitious matrix was investigated thanks to a parametric study by modifying the ratio between the width and the thickness of the rectangular perimeter. Djamai et al. [5] carried out multi-scale numerical modeling for the TRC sandwich panel from the micro-scale (pull-out response of textile yarn from cementitious matrix block) to macro-scale (TRC sandwich panel in four points bending test). This multi-scale model could take into consideration all the possible mechanisms of failure of its constitutive materials (concrete cracking and concrete-textile debonding). Rambo et al. [6] used a finite-difference model to simulate the residual tension stiffening behavior of TRC specimens after exposure to the elevated temperature of pre-heating. This model could present the effect of the bond-slip relationship on the crack spacing as well as stress-strain curves at different temperatures. This research was based on different methods and provided the results in good agreement with that of the experiment. They also have significantly contributed to our knowledge of numerical modeling on the mechanical behavior of TRC composite. However, the disadvantage of these models' is cannot show the failure mode with multi-cracks on the surface of the cementitious matrix as in experimental results.

In the stress-train relationship of TRC composite, the cracking of the cementitious matrix progressively occurs corresponding to the second phase. Due to the complex response of the cracked cementitious matrix, it can significantly affect the local and global behavior of TRC composite. In the experiment, the mechanical behavior of the cementitious matrix in the cracked and uncracked regions, obtaining by the contact measurement methods, was different [7]. Furthermore, the global behavior of the TRC composite strongly depended on the length and position of the measurement zone.

Until now, a big question for the numerical approaches of the mechanical behavior of TRC composite under tensile loading is how to model the cracking of the cementitious matrix. Regarding the cracking model for the cementitious matrix, in the literature, there were two main approaches to simulate the non-linear behavior considering its crushing and cracking [8]. The first one was the discrete cracking approach in which the crack was considered as a discontinuity of the material at its position. However, the limit of this approach is the need to use automatic re-meshing techniques that then make it possible to model cracks dividing the elements of the initial mesh. The second was a homogenized approach that gives a global behavior of the cementitious matrix in tension without taking account of the explicit opening of cracks [8]. Thus, it allows keeping the original mesh and does not impose constraints a priori on the orientation of the cracks [9].

To the best of the authors' knowledge, no numerical results are available concerning the effects of the cracking and the influence of the length and position of the measurement zone on TRC's global response. Thus, this paper presents numerical results of 3-D modeling of TRC composite in which the nonlinear behavior model was used by considering the cracking of the cementitious matrix. The numerical results will be compared and discussed in this paper to find agreement with the experiment

data in the literature. A parametric study could show the effect of several studied parameters belonging to the test setup process as the length and position of the measurement zone.

2. Numerical model

This section presents all numerical procedures, including the element type choice, the material model used, experimental data, meshing, boundary conditions, and loading. Firstly, the 3-D model was created in the ANSYS software to validate the experimental results on F.GC1 composite in ref [10]. Afterward, a parametric study would be carried out from this model by modifying the mechanical properties of component materials as presented in previous studies.

2.1. Element types

In this numerical study, two types of elements were used for the component materials. The first chosen one for the reinforcement textiles was LINK180 (3-D Spar or Truss). It is a uniaxial element of tension (or compression) with three degrees of freedom at each node: translations in the nodal directions x, y, and z (see Fig. 1(b)). Second, SOLID65 (3D Reinforced Concrete Solid) was chosen for the cementitious matrix. It allows the presence of different materials like steel or textiles to generate a composite material (TRC composite in this case). Particularly, this material model is capable of cracking when it is under tensile loading. Fig. 1 below shows both elements in the 3D numerical model for the TRC composite.

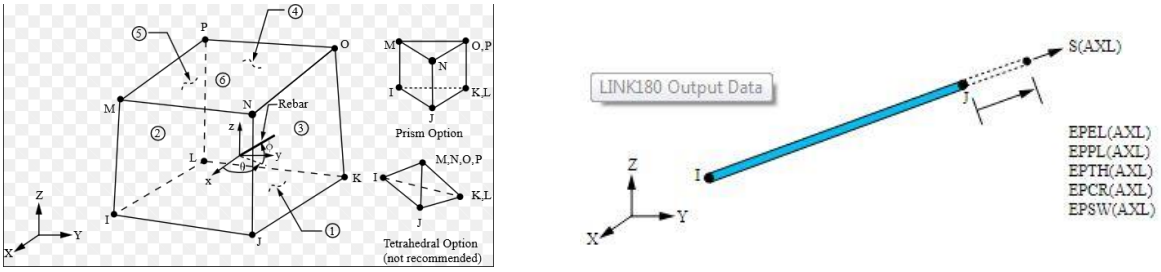

(a) SOLID65 element for concrete matrix

(b) LINK 180 element for carbon textile

Figure 1. Element types used in the numerical model [11]

2.2. Material model

The material models used for the TRC composite components in this study based on their mechanical behavior and corresponded to each element type. Regarding the material model for reinforcement textiles, the perfect linear elastic model was chosen to simulate its work under tensile loading. The principal parameters of this material model are the ultimate strength and Young's modulus. For the cementitious matrix, the concrete model (CONCR - Nonlinear Behaviour - Concrete) [12] was chosen. It can present the failure mode of fragile materials such as concrete, stone, ceramics, and cracking failure is considered.

The criterion for failure of concrete due to a multiaxial stress state can be expressed in the following equation (proposesd by Willam and Warnke [7]):

$$\frac{F}{f_c} - S \geq 0 \tag{1}$$

where F is a function of the principal stress state ($\sigma_{xp}, \sigma_{yp}, \sigma_{zp}$), depending on the failure surface. S is failure surface expressed in terms of principal stresses and five input parameters f_t (ultimate uniaxial tensile strength), f_c (ultimate uniaxial compressive strength), f_{cb} (ultimate biaxial compressive strength), f_1(ultimate compressive strength for a state of biaxial compression superimposed on hydrostatic stress state) and f_2 (ultimate compressive strength for a state of uniaxial compression superimposed on hydrostatic stress state), f_c is uniaxial crushing strength. If the mentioned equation above is satisfied, the material will crack or crush.

Fig. 2 shows the stress-strain relationship of this model in the case of cracking in one direction only as TRC composite, where f_t is uniaxial tensile cracking stress; T_c is multiplier for the amount of tensile stress relaxation; ε_{ck} is uniaxial tensile cracking strain; R_t is slope (secant modulus).

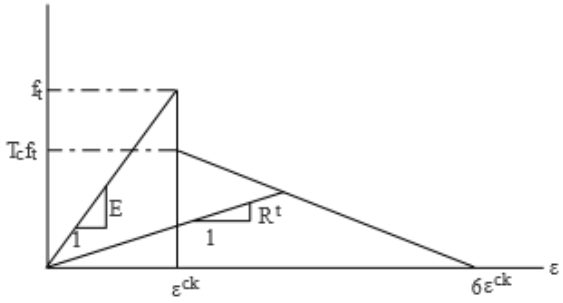

Figure 2. Stress-strain relationship of the cracked condition (CONCR – Nonlinear Behavior – Concrete) [11]

2.3. *Experimental data*

The data based on the experimental results concerning the tensile behavior of TRC composite were chosen for this study. Firstly, the experimental data on carbon TRC in Ref. [10] were used to validate the numerical model. In this study, the GC1 and GC2 carbon textile was combined with refractory concrete to respectively manufacture F.GC1 and F.GC2 composites for characterization at different temperatures. However, only result at room temperature was used for the validation of the

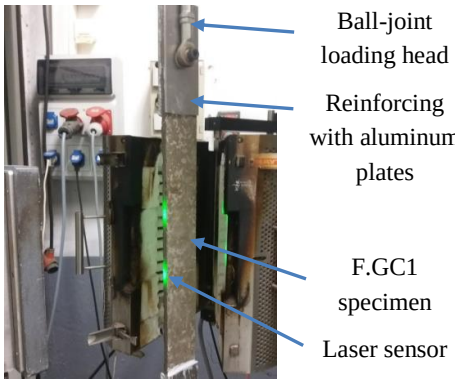

(a) Test setup for carbon TRC specimens

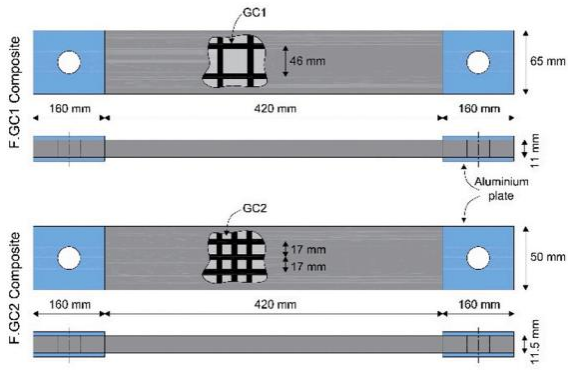

(b) Dimentions of both TRC specimens

Figure 3. Experimental works for the validation of 3-D model [3, 10]

3-D model. The tensile tests were carried out on both carbon TRC specimens, as shown in Fig. 3(a). Afterward, this model was used to predict and compare the global mechanical behavior of TRC composite in another research, as presented in Table 1.

Table 1. Experimental data used in the numerical model

Experimental data	Reinforcement textile			Cementitious matrix				
	Describe of materials	E_f (GPa)	σ_f (MPa)	Describe of materials	E_m (GPa)	f_t (MPa)	ε_{ck}	T_c (MPa)
F.GC1 of Tran et al. [10]	Carbon textile	144	1312	Refractory cementitious matrix	8.41	5.29	6.29×10^{-4}	0.8
F.GC2 of Tran et al. [10]	Carbon textile	144	1312	Refractory cementitious matrix	8.41	5.29	6.29×10^{-4}	0.8
M2-G-1L of Saidi and Gabor [7]	AR Glass textile	35	520	Self-placing cementitious matrix	14	4.5	3.21×10^{-4}	0.8
Basalt TRC of Rambo et al. [6]	Basalt textile	43.2	688	Refractory cementitious matrix	34	3.5	1.03×10^{-4}	0.8

2.4. Meshes, boundary conditions and loads

The specimen in the numerical model was created step by step with Ansys APDL 2015, corresponding to half of the corresponding dimension of the F.GC1 specimen in ref [10] (11mm × 65mm × 370mm) (see Fig. 3(b)). The block of the cementitious matrix was meshed in parallelepiped form by the SOLID65 elements with the size depending on that of each edge of the model. The reinforcement textile was created and meshed as a truss bar by the LINK180 elements.

Concerning the boundary conditions and loads, all the nodes in the talon part of the first end were fixed supports with all movements blocked according to three coordinated axes. This zone corresponded with that one bonded with the aluminum plates to reinforce the cementitious matrix elements, ensuring the fixed supports of the elements in this zone. The mechanical load was applied to the other end of the specimen by the imposed displacement with the speed of the applied load as in the experiment. Fig. 4 shows the boundary condition and loading configuration for the numerical model.

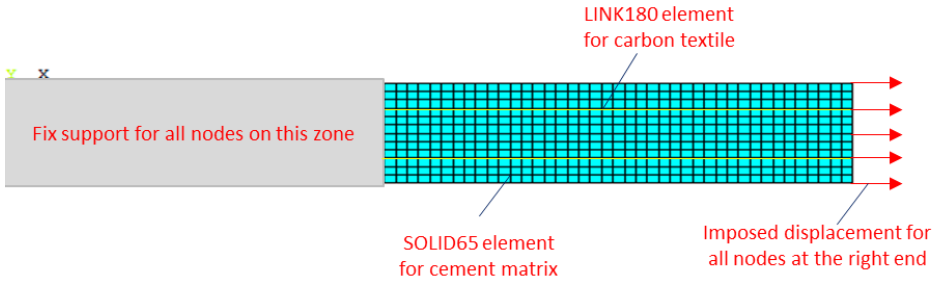

Figure 4. Configuration of meshing, boundary conditions and loads for the glass TRC specimen model

3. Numerical results

3.1. Mechanical behaviour of carbon TRC composite

Fig. 5 presents the stress-strain relationship of the F.GC1 composite obtained from a 3-D numerical model in comparison with experimental results. As result, the 3-D model could present a strain-hardening behaviour of carbon TRC composite with four states as in the literature. In the first one, the un-cracked material behavior where the reinforcement contribution is negligible, and the linear slope represents the elastic modulus of the concrete. In the second, the translation between the first state and second state is indicated by the apparition and development of the first cracks in the concrete matrix. In this stage, the load transfers from the cement matrix to the textile filament and redistributes step by step. In the next one, the concrete support is negligible and only the textile filament resists the load. In this period, the cracks are kept widening with the elastic modulus of textile until reaching its ultimate collapse. Finally, the pattern of this failure is maybe brittle or plastic behavior, depend on many factors such as fabric geometry, reinforcement ratio, and the bond strength in the fourth period. From Fig. 5, it could be observed the cracking phase by the drops in stress as in the experiment.

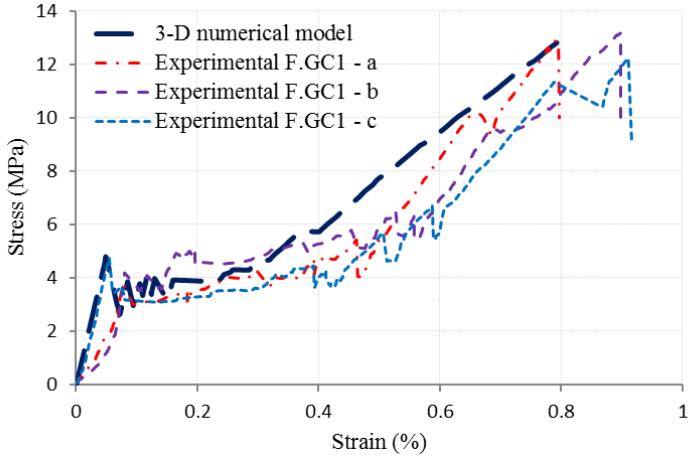

Figure 5. Stress – strain relationship of tensile behaviour of F.GC1 specimens in compairison with experiment

The mechanical properties of carbon TRC were identified from this stress-strain curve. In comparison with the carbon TRC's mechanical properties obtained from the experiment, this 3-D model presents an interesting agreement, particularly in the first and third phase. In the first one, the cracking stress (σ_I) and the first Young's modulus (E_I) were respectively 4.78 MPa and 10.73 GPa for the 3-D model, compared with 4.25 MPa and 10.57 GPa for the experiment. It could be found that there was a difference in the first stage between both experimental and numerical results (specimens F.GC1 - a and F.GC1 – b with the 3-D model). It was belonging from the errors of the preparation procedure of TRC specimens in the experiment. In the third one, comparative value pairs between both experimental and numerical results were respectively 12.76 MPa and 13.09 MPa for the ultimate strength (σ_{UTS}), 0.866 %, and 0.806 % for ultimate strain (ε_{UTS}).

However, when comparing experimental and numerical results in the cracking phase, the length of this stage is inconsistent between them (see Fig. 5). This difference is due to the effect of the dynamic phenomena after each crack appearance on the experimental strain measured. After each time that the cementitious matrix reaches its limit, cracks will occur somewhere in the specimen. This leads to a

decrease in the tensile force and causes a dynamic effect on the specimen where the crack occurs. Meanwhile, the reinforcement textile will be pulled out from the cementitious matrix and cause an increase in the overall deformation of the sample. This will prolong the cracking phase (Stage 2) on the stress-strain curve.

When using this 3-D model for other TRC materials in previous experimental studies, it can see a good agreement between both numerical and experimental results. Table 2 below presents the comparison for the mechanical properties of TRC composites in the first and third phase between experimental and numerical results.

Table 2. Comparison between both experimental and numerical results

Results		1^{st} phase		3^{rd} phase		
		σ_I (MPa)	E_I (GPa)	σ_{UTS} (MPa)	ε_{UTS} (%)	E_{III} (GPa)
F.GC1 - Tran et al. [10]	Numerical	4.78	10.73	13.09	0.806	1.78
	Experimental	4.25	10.57	12.76	0.866	3.04
F.GC2 - Tran et al. [10]	Numerical	5.31	11.29	10.95	0.889	1.43
	Experimental	6.38	11.33	10.30	0.813	2.50
M2-G-1L - Saidi and Gabor [7]	Numerical	4.23	13.67	11.02	1.542	0.32
	Experimental	4.64	13.10	10.30	1.333	0.49
TRC bazan - Rambo et al. [6]	Numerical	3.58	34.25	13.98	1.62	0.89
	Experimental	3.45	34.64	13.49	1.58	0.67

3.2. Stress and strain distributions

Along with the identification of the overall stress-strain curve of the TRC specimen, the 3-D model also allows showing the stress and strain distribution in the reinforcement textile, as well as the cementitious matrix at each step of numerical calculation. For the cementitious matrix, Fig. 6(a) shows the distribution of axial displacement at the last calculation step. It can be found that, due to the presence of the textile yarns, this displacement and deformation at points on the same cross-section are not equal. All nodes with the same displacement form wavy contour lines, as shown in Fig. 6(a). For the carbon textile yarns, the axial stress is similar in the part where the TRC specimen was subjected to tensile load. At the end of the sample that was bonded with aluminum plates, the stress on the textile yarns is relatively small. This result is in agreement with the experiment because these sections have been reinforced by bonding with aluminum plates. Fig. 6 below presents the stress and displacement distribution on the TRC specimen at the last step of numerical calculation.

3.3. Failure mode

As the numerical results obtained, the 3-D model can show the failure mode of the carbon TRC specimens with transverse cracks along its length, as shown in Fig. 7(a). Transverse cracks along the TRC specimen's length began at locations with carbon textile yarns, and the spacing between two cracks are relatively evenly spaced. These results are in good agreement with the experimental results by observing the TRC specimens after testing (see Fig. 7). So, it could be said that the material model for the cementitious matrix has correctly reflected its working in TRC composite. This material

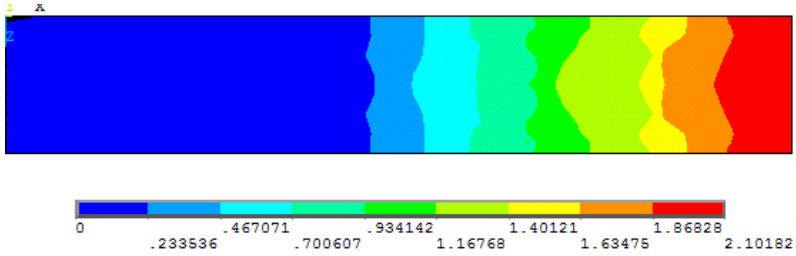

(a) Distribution of axial displacement in F.GC1 specimen

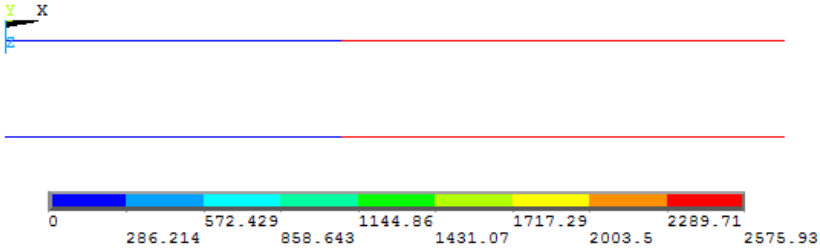

(b) Distribution of axial stress in GC1 textile

Figure 6. Stress and strain distribution in carbon textile and cementitious matrix of F.GC1 specimen at the last step of numerical calculation

model has been considering the material failure due to cracking or crushing for the cementitious matrix. Besides, the 3-D model also allows observing the formation and development of cracks from a microscopic crack appearing at one element of the model to a macro-crack in the cross-section.

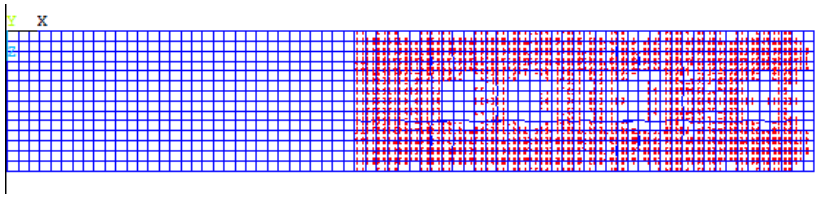

(a) Failure mode of F.GC1 in 3-D numerical result

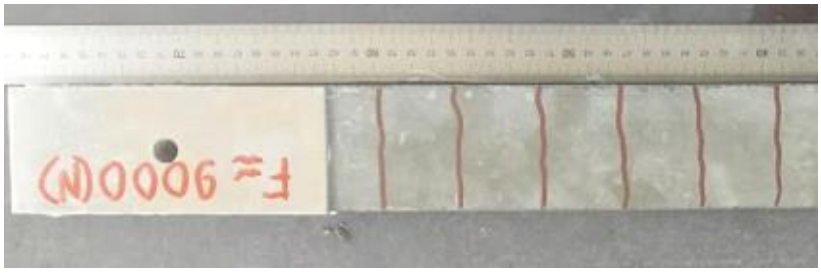

(b) Failure mode in the experiment

Figure 7. Comparison of the failure modes of carbon TRC specimens between both experimental and numerical results

4. Discussion

4.1. Effect of deformation measurement length

In the experiment, the deformation measurement method is the main factor for the characterization of the global mechanical behavior of TRC composite. So, the length of this deformation measurement, and its location could influence the shape of the stress-strain curve. Fig. 8 presents the stress-strain curves of three cases of deformation measurement length from 5 cm to 21 cm on the surface of the TRC specimen. It could be found that in the case of 5cm in the middle, all previous cracks were not recorded in the stress-strain curve (see Fig. 8(a)). So, it needs to modify by a technic for the cracking phase of the mechanical behavior of TRC composite proposed in Ref. [6]. The modified curve was in good agreement with experimental data for F.GC2 composite in Ref. [9] (see Fig. 8(b)). With the deformation measured length longer, the stress-strain curves were like idealized ones, as analyzed in [6]. The cracking phase was described by the drops in stress, and the stress in the next crack is

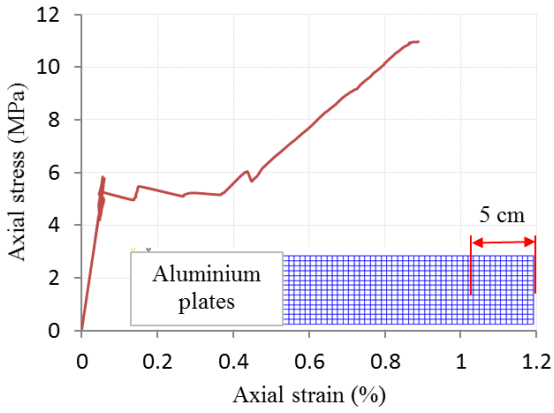

(a) Deformation measured length of 5 cm in the middle

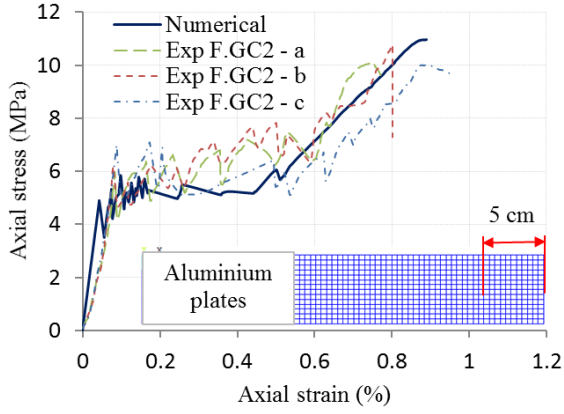

(b) Deformation measured length of 5 cm (modified version)

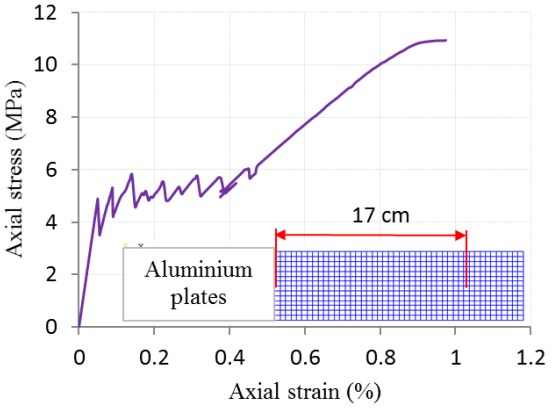

(c) Deformation measured length of 17 cm

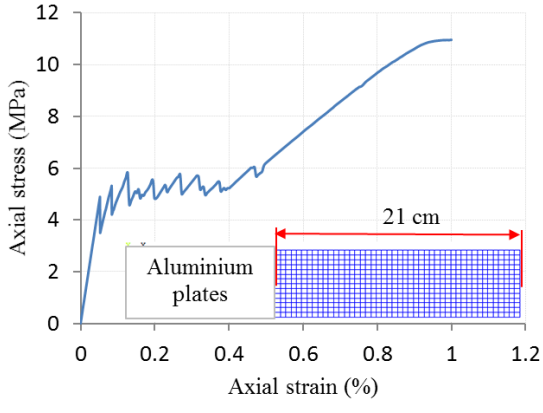

(d) Deformation measured length of 21 cm on all surface of a haft specimen

Figure 8. Effect of deformation measured length on stress-strain curve of mechanical behaviour of TRC composite

higher than the previous (see Figs. 8(c), 8(d)). So, it could be said that the length of deformation measurement is the longest it if possible, for the characterization of TRC's mechanical behavior.

4.2. Development of cracking zone

Fig. 9 below shows the process of cracking zone widening on the surface of the TRC specimen from non-cracking to the stabilization of cracks. The first crack always occurred in the cross-section next to the fixed support zone. This could be explained by the effect of dynamic phenomena as well as that of the concentration in stress when the specimen was subjected to the tensile force. This process in the 3-D model was relatively ideal, meaning that the crack occurred sequentially from the outside to the inside. The widening of the cracking zone occurred beginning from the redistribution of tensile efforts from carbon textile yarns to cementitious matrix after the first crack. This process happened and caused the cracking for the matrix elements (SOLID65) connecting with the textile yarn one (LINK180). It continued until the next crack, as presented in Figs. 9(b), 9(c). In comparison with

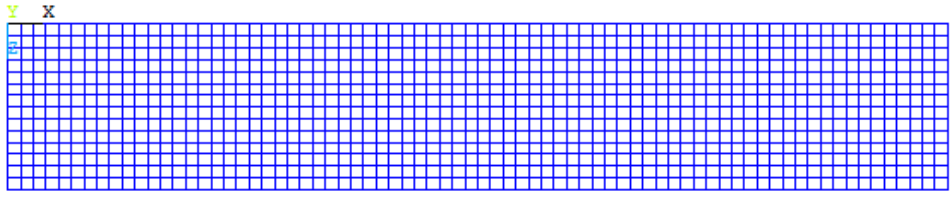

(a) Non-cracking on specimen

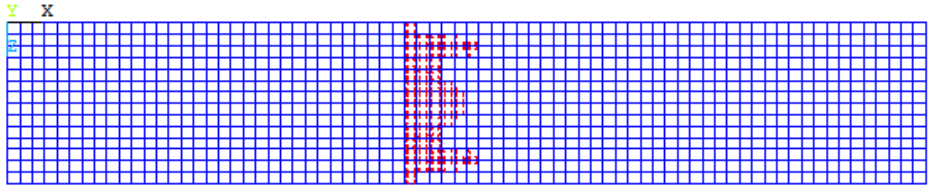

(b) Complete crack on a cross-secion

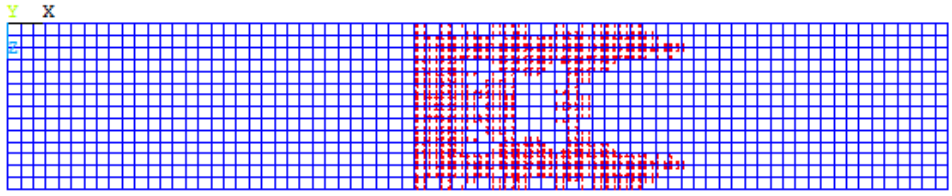

(c) Widening of cracking zone on the TRC surface

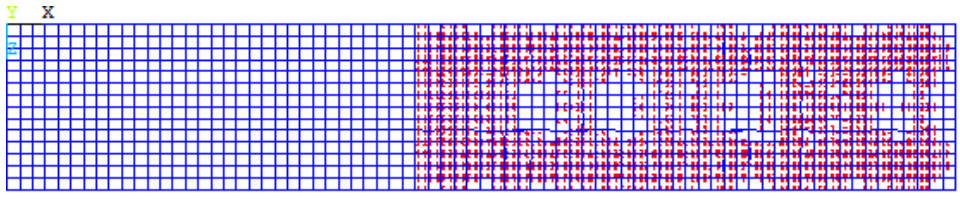

(d) End of cracking phase with multi-cracks on the surface

Figure 9. Development of cracking zone on the surface of TRC specimen

this observation in the experiment, there is a little difference between them. In the experiment, the crack occurred more randomly, depending on the uniformity of the cementitious matrix of the TRC specimen. However, the spacing between the cracks still has ensured the criticals related to the load transmission length (δ_0), as mentioned in [7]. Thus, as presented in Section 3.3, the 3-D model allows showing the failure mode in agreement with the experimental result.

4.3. Disavatage of 3-D model

It could be found that the 3-D model gives relatively accurate results on the mechanical behavior of the TRC materials when compared with the experimental results. However, this model assumes that the surface bonding between the textile reinforcement and the cementitious matrix was perfect. In some case studies as corrosion or at high temperatures, the together working between the two material layers at the interface surface is not as hypothesized, leading to a significant difference between numerical and experimental results. Furthermore, this model just corresponds with the TRC composite with the reinforcement of continuous fiber. In the case of reinforcement with discontinuous fiber, it needs to use the method of equivalent conversion from the reinforcement ratio for calculation steps.

5. Conclusions

In this numerical study, a 3-D finite element model was developed and validated from experimental data to predict the mechanical behavior of the TRC composite at mesoscale. The following conclusions can be drawn from the numerical results:

- The 3-D numerical model presented exciting results concerning the stress-strain relationship and failure mode of the TRC specimen. It could simulate the cracking phase of TRC's behavior by using the non-linear behavior considering the crushing and cracking for the cementitious matrix. The TRC specimen also presented the failure mode with the transversal cracks on its surface.

- The 3-D numerical model could predict the mechanical properties of the TRC specimen. In comparison with the experimental data, there was a good agreement between both experimental and numerical results, especially in the first and third phases of the mechanical behavior of TRC composite.

- From the 3-D numerical model, could be observed the stress and strain distribution on TRC specimen at each calculation step, also progress of the development and widening of cracks on its surface. Hence, the influence of the deformation measurement length and its position on the stress-strain curve could be found, essentially relating to the cracking phase and then changing the global strain.

- The 3-D model still has some disadvantages belonging from the assumption of the perfect bonding between the reinforcement textile and the cementitious matrix. This model just corresponds with the TRC composite with the reinforcement of continuous fiber. In the case of discontinuous fiber, it needs to use the equivalent conversion method for the numerical calculation.

Acknowledegment

This research has been performed with financial support of the Ministry of Education and Training of Vietnam thought the project B2021-MDA-10.

References

[1] Thach, L., Dung, P. C., Tung, B. T., Thao, D. T., Tung, N. G. (2019). Research to determine basic parameters of fiber reinforced concrete extruder. *Journal of Science and Technology in Civil Engineering (STCE) - NUCE*, 13(3V):84–90. (in Vietnamese).

[2] Tran, T. M., Do, T. N., Dinh, H. T. T., Vu, H. X., Ferrier, E. (2020). A 2-D numerical model of the mechanical behavior of the textile-reinforced concrete composite material: effect of textile reinforcement ratio. *Journal of Mining and Earth Sciences*, 61(3):51–59.

[3] Tran, M. T., Vu, X. H., Ferrier, E. (2020). Mesoscale numerical modeling and characterization of the effect of reinforcement textile on the elevated temperature and tensile behaviour of carbon textile-reinforced concrete composite. *Fire Safety Journal*, 116:103186.

[4] Portal, N. W., Thrane, L. N., Lundgren, K. (2016). Flexural behaviour of textile reinforced concrete composites: experimental and numerical evaluation. *Materials and Structures*, 50(1).

[5] Djamai, Z. I., Bahrar, M., Salvatore, F., Larbi, A. S., Mankibi, M. E. (2017). Textile reinforced concrete multiscale mechanical modelling: Application to TRC sandwich panels. *Finite Elements in Analysis and Design*, 135:22–35.

[6] Rambo, D. A. S., Yao, Y., de Andrade Silva, F., Filho, R. D. T., Mobasher, B. (2017). Experimental investigation and modelling of the temperature effects on the tensile behavior of textile reinforced refractory concretes. *Cement and Concrete Composites*, 75:51–61.

[7] Saidi, M., Gabor, A. (2020). Iterative analytical modelling of the global behaviour of textile-reinforced cementitious matrix composites subjected to tensile loading. *Construction and Building Materials*, 263: 120130.

[8] William, K. J., Warnke, E. P. (1975). *Constitutive model for the triaxial behaviour of concrete*.

[9] Truong, B. T. (2016). *Formulation, performances mécaniques, et applications, d'un matériau TRC pour le renforcement et la réparation de structures en béton/et béton armé: Approches expérimentale et numérique*. Phdthesis in French, Université de Lyon.

[10] Tran, M. T. (2019). *Caractérisation expérimentale et modélisation numérique du comportement thermomécanique à haute température des matériaux composites renforcés par des fibres*. Phdthesis in French, Université de Lyon.

[11] ANSYS (2011). *Mechanical APDL Element Reference 14*. ANSYS Inc.

[12] Kohnke, P. (2009). *Theory Reference for the Echanical APDL and Mechanical Applications*. ANSYS Inc.